한국기계가공학회지, 제19권, 제7호, pp.89～97(2020.07) ISSN 1598-6721(Print)
Journal of the Korean Society of Manufacturing Process Engineers, Vol. 19, No. 7, pp.89~97(2020.07) ISSN 2288-0771(Online)

https://doi.org/10.14775/ksmpe.2020.19.07.089

A Study on the Variation of Physical Properties of Line-heated for Type-B LNG Fuel Tank with 9% Nickel Steel Plate

Kyung-Shin Choi*, Ji-Han Lee*, Ji-Ung Hong**, Won-Jee Chung***,#
*Lloyds Register, **HYUNDAI SAMHO HEAVY INDUSTRIES CO.,LTD., ***Changwon National University

9% Nickel강이 적용된 Type-B LNG 연료탱크 선상가열의 물성 변화에 관한 연구

최경신*, 이지한*, 홍지웅**, 정원지***,#
*로이드선급, **현대삼호중공업, ***창원대학교

(Received 03 February 2020; received in revised form 17 April 2020; accepted 13 May 2020)

ABSTRACT

Container vessels continue to grow in size, led by global shipowner. Large ships can be loaded more cargo at a time, reducing the cost of transportation per teu. this eventually leads to economies of sale, in which the production cost per unit decreases with increasing output. in accordance with the 70th Convention of the Marine Environment Protection Committee of the International Maritime Organization, as of January 1, 2020, MARPOL Annex Ⅵ Regulation 14.1.3 will be effective. All vessels must be meet these criteria to reduce Sox emissions and reduce NOx emissions by reducing the content of manned sulfur oxides from 3.5% to less than 0.5%, otherwise IACS Member States Entry to the port is denied. in order to do that need to LNG storage tank. in this study characteristic of the material after line heating (600℃,700℃,800℃,900℃) of 9% Ni steel used in the manufacture of LNG fuel tank of ship were verified using by mechanical test. In the heating method by line heating. The initial properties of steel are changed by variables such as temperature, time, speed. The experimental data of line heating presented in this paper confirmed that the initial change of 9% Ni steel could be minimized.

Keywords : Line-Heating(선상가열), Heat Affected Zone(열 영향부), Finite Element Analysis(유한요소해석), Distortion(뒤틀림), Thermal Conduction(열전도), Root Gap(루트간격)

1. Introduction

The trend towards increasing the scale of ships is costly as fuel use significantly increases accordingly. Additionally, large amounts of sulfur oxides (SOx) may be the main source of marine air pollution due to the increased use of Bunker C oil, which is commonly used as ship fuel. Accordingly, the International Maritime Organization (IMO) will be subject to the IMO 2020 Convention. The main objective of the IMO 2020 agreement is to reduce the content of SOx in bunker fuel from less than 3.5 % to less than 0.5 %, thereby preventing the

Corresponding Author : wjchung@chanwon.ac.kr
Tel: +82-55-213-3624, Fax: +82-55-263-5221

release of SOx causing acid rain and reducing emissions of nitrogen oxides (NOx). Furthermore, to deny entry to ships that do not comply with these standards to ports of the member countries of the International Association of Classification Societies (IACS). According to recent studies, three major alternatives are being considered to reduce SOx emissions: first, a method to substitute low-sulfur oil fuel; second, the installation of a scrubber, i.e., a method of installing a device to reduce emissions of SOx in ships; and finally, the possibility of designing ships powered by liquefied natural gas (LNG). In particular, with the introduction of LNG-fueled propulsion ships, the emission of SOx can be eliminated by 100 % compared to conventional bunker fuel. If the engine operates on a four-stroke cycle, non-sulfur environmental pollutants can also be greatly reduced by a 90 % reduction in NOx, a 90 % reduction in fine particulate matter (PM), as well as a 15 % decrease in carbon dioxide (CO2). This refers to the useful function of installing a separate LNG tank inside the ship to supply LNG to the ship. Currently, container ships equipped with type-B LNG propulsion tanks made with 9 % nickel steel are being built. Their purpose is to cool the LNG to the cryogenic temperature of -163°C, liquefying the volume ratio to 1/600; thus, maximizing transportation efficiency. In the case of 9 % nickel steel, the mechanical properties at cryogenic temperatures have been verified by various studies. However, no proper verification has yet been made concerning line heating at weld zones. Generally, when making curved hull surfaces, there are ways to use cold working, i.e., roll bending or pressing, and to heat certain parts of the curved surfaces with line heating and triangular heating to use contraction and bending[1]. Line heating causes different internal structural transformations in steel due to its characteristics, type and strength of heat source, heating time, and speed. Additionally, if these variables intervene, the steel may change its initial properties. Thus, the rigidity considered from the design phase may change, resulting in the loss of the function of the structure, creating safety issues[2-4]. In this regard, Jae-won Kang and others conducted a study to evaluate the strength of LNG storage tanks[5]. Additionally, the residual stress of the weld zones in the 9 % nickel steel thick plate was actively studied[6].

In this study, after line heating was applied to the weld zones of the storage tanks made of 9 % nickel steel, it was verified through experimentation whether the classification guidelines were satisfied while maintaining the characteristics of the material through tensile, hardness, and impact tests. This study was conducted to analyze the deformation caused by line heating in the current shipyard through thermal analysis and to develop measures to optimize it.

2. Experimental Conditions and Methods

2.1 Application of 9 % Nickel Steel Thick Plates

LNG tanks are spherical and have a stand-alone type-B tank consisting of a self-supporting prismatic tank, support blocks, and insulation panels designed using precision strength calculations, analysis, and model experiments. Generally, these tanks are made of 5083-0 aluminum and are divided into four sections by the swash bulkhead and the longitudinal bulkhead. To reduce sloshing, the large girders installed on the external walls are configured to prevent liquid flow in advance on the external walls, which act as water-tight boundaries. The heat dissipation material consists of a polyurethane foam panel reinforced with glass fiber, which is pre-made in the factory and attached to studs outside the tank. These systems are designed to have separate heat dissipation panels; additionally, flexible cushion

Table 1 Chemical composition of 9% Nickel steel

Steels	C	Si	Mn	P	S	Cu	Ni	Cr	Mo	T.Al
YP 655	0.75	0.22	0.65	0.003	0	0.02	9.07	0.01	0.04	0.023

Table 2 Mechanical properties of 9% Nickel steel

Steels		Tensile Strength (N/mm2)	Elongation (%)	Y.R (Yield Ratio) (%)
YP.655	11~12mm	720	25	91

joints are inserted between the panels to absorb contractions and expansions. However, if heat is generated due to welding work during the manufacturing process of the cargo window, the temperature rises above the A1 transformation temperature for a certain period and then cools down, resulting in problems caused by changes in material properties whereby the strength decreases. LNG carriers use materials such as aluminum 5083-0 and stainless steel. However, the properties of these materials increase with thickness owing to the low yield strength of aluminum. Approximately 117 MPa for aluminum and 220 MPa for stainless steel, resulting in higher material prices. In particular, the proof stress (or yield strength) for pitting corrosion is weak when the iron is contaminated. As an alternative to this improvement, nickel is added to the steel while the tank is being manufactured to prevent cold brittleness (or cold shortness) and improve flexibility, which results from the improved hardenability of the heat treatment properties i.e. nickel improves the harness of steel through its thermal properties. Table 1 shows the chemical composition of 9 % nickel steel.

Table 2 shows the mechanical properties of 9 % nickel steel as indicated by the manufacturer.

2.2 Application and Location of Line Heating

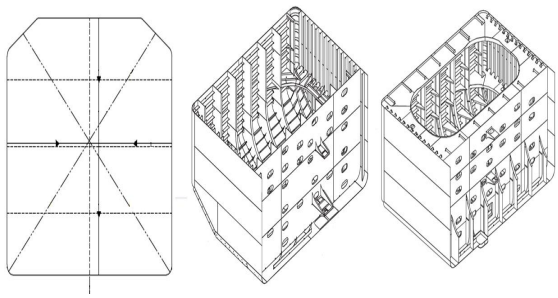

Fig. 1 Block division of type-B LNG tank

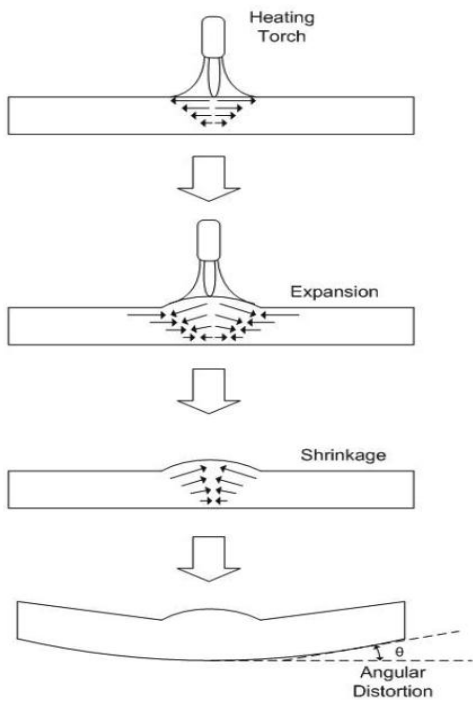

Fig. 2 Mechanism of plate forming by line heating[8]

The 9 % nickel steel type-B LNG fuel tank currently under construction is shown in Figure 1. This fuel tank is located at the bow of the ship Frame 88+1720, starting from the stern of the ship Frame 80+2300. The tank is 24.4 m long, 26.3 m wide, and 22.9 m high; additionally, the upper and lower parts of the tank are manufactured separately. By dividing left and right from the center of the tank, a total four-sections of erection-method was

adopted. In addition, the main experimental target of line heating is the external plate part of the tank, as the external member is more likely to change the curvature volume than the internal member; therefore, the line heating method must be applied primarily to correct this[7].

Plate bending by line heating is a method of heating one side of a plate with heat, creating a temperature gradient in the direction of the thickness, and bending the plate according to the plasto-elastic deformation caused by the temperature gradient. Figure 2 is a step-by-step representation of the mechanism of forming steel plates by line heating, where the angular deformation θ can be obtained as shown in Expression 1 as the free-end rotational angle:

$$\theta = \arctan\left(\frac{M}{EI} * a\right) \quad (1)$$

Where E is the modulus of elasticity of the material, I is the cross-sectional quadratic moment, α is the arm length of the moment (one-half the width of the heating), and M is the bending moment. If Expression 1 is substituted for the second section moment, it can be represented as Expression 2.

$$\theta = \arctan\left(\frac{a}{b} * \frac{M}{Et^3} * 12\right) \quad (2)$$

Assuming a micro-angle deformation, the above expressions can be represented by Expression 3. In addition, the relationship between the bending moment M and the angular deformation volume θ is as shown in Expression 4.

$$\theta = \left(\frac{M}{Et^3} * 12\right) * \left(\frac{a}{b}\right) \quad (3)$$

$$M = \left(\frac{b}{a}\right) * \left(\frac{Et^3}{12}\right) * \theta \quad (4)$$

Therefore, when the relationship between the angular deformation volume and the input heating volume is defined as $\theta = k \cdot Q/t^2$, the input heating volume and the bending moment are as shown in Expression 5.

$$M = \left(\frac{t}{12} * E\right) * \left(\frac{b}{a}\right) * (Q * \kappa) \quad (5)$$

2.3 Welding Technique and Line-Heating Sequence

Table 3 shows three welding specifications and conditions regarding the thickness of the material applying the butt-welding technique. The shape of the weld was applied with an improvement angle between 50 and 80 degrees, a maximum distance of 2 mm of the root face interval, and 0 to 8 mm of the root gap. The special features for the welding conditions are as follows.

1) If air temperature is below 0 °C, pre-heat to a minimum of 20 °C.
2) Sufficient dryness should be maintained.
3) Preheating temperature should be applied according to the classification guide.
4) Preheating should be done with a torch and a heating pad.
5) Magnetization should be measured with a calibrated gaussmeter before welding.
If magnetization exceeds 300 gausses, perform welding after demagnetization.

Some of the factors affecting the magnitude of the bending moment caused by line heating of the welds in LNG tanks include the type of heat source, temperature, moving speed, material properties of the plate, geometrical shape and thickness of the plate, and cooling method. In this paper, the line heating method is used to generate plate bending by using gas as the main heat source on the plate surface. The plate is heated in a straight

Table 3 Typical welding parameters for butt joint with single V-bevel

Pass	AMP [A]	VOLT [V]	Welding Speed [Cm/Min]	Heat Input [KJ/Cm]	Welding Position
1st	145~180	28~32	13.4~22.3	12.1~20.3	
Fill	160~200	28~32	13.5~37.5	8.8~14.8	1G
Cap	160~200	27~32	18.9~36.4	8.7~14.6	
1st	145~175	23~27	7.1~11.8	19~31.8	
Fill	150~200	26~31	18~50	6.4`10.8	2G
Cap	160~200	26~30	31.3~59.5	5.1~8.6	
1st	135~165	21~25	5.6~9.4	20.6~34.4	
Fill	150~190	24~28	7.4~16.9	17.5~29.3	3G
Cap	150~190	24~28	7.3~14.4	18.9~31.5	

Table 4 Heating temperature for 9% Nickel steel

Plate	Cooling method	Temperature (℃)	Manual speed (Cm/Min)	Carriage speed gauge
9% Ni Steel	Air Cooling	600	75~65	4.3~5.0
		700	65~45	3.5~4.3
		800	30.6~28.3	3.4~3.7
		900	16.9~15.6	2.7~3.0

line or an arbitrary curve and then cooled naturally. The heating temperatures used in the LNG tank welds were divided into 600, 700, 800, and 900 °C, based on the results of an experiment that showed no degradation in the mechanical properties, even when the temperature was decreased, after heating up to 900°C without distinction of steel [9]. Table 4 shows the speed of the heating torch according to the heating temperature distribution when the heating position is 10 to 30 mm away from the welded part. A digital thermometer was used to measure the temperature 50 mm away from the heated zone.

2.4 Structural Analysis Model

ANSYS, a commercial analysis software, was used to measure the temperature distribution and

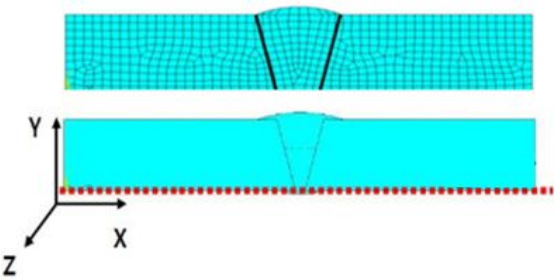

Fig. 3 FE analysis single V-bevel 50 to 80 angle degree

gradient of the weld zones. To determine the deformation volume using heat distribution as the thermal load after the heat transfer analysis, the modulus of elasticity 2.1 kg/cm², Poisson ratio 1/m=0.31, coefficient of thermal conductivity (which is a proportional constant in conduction) 60.7W/m-k, and the specific heat applied to the unit mass were determined within the elastic domain with a material value of 0.460 J/g-°C. The mechanical welding deformation of structural analysis results was analyzed and the mechanical characteristics of the weld zones in the single V-shaped bevel of the butt joints were identified. Figure 3 shows the modeling forms (or geometrical shapes) of the weld zones according to the shapes of the beveled surfaces. The previously mentioned two-dimensional unsteady static heat conduction analysis was performed on the thermal properties of the butt weld zones of 9 % nickel steel. The numerical analysis was carried out taking into account the temperature table for multi-layer or more than two-pass layer welding method as soon as the welding began. Additionally, line heating analysis of the weld deformation was determined as a function of the distribution and size of the unique deformation around the weld zones using temperature distribution according to temperature change.

3. Experimental Results and Considerations

Table 5 Tensile test results for welding butt joint

Sample	Thickness (mm)	Width (mm)	Max Load (N)	Tensile Strength (N/mm2)
1A-1	11.0	25	206221	711
1A-2	11.0	25	205835	709
2A-1	12.0	25	230714	769
2A-2	12.0	25	231512	771

3.1 Tensile Test Results of Weld Zones

Tensile strength tests were carried out to ensure the safety of the weld structure as weld zones are likely to be weak in the heat-affected zones (HAZs) produced by the thermal effects of welding. Furthermore, they may have defects near the fusion or melting point of the weld metal. Table 5 shows the maximum load and tensile strength values at the time of fracture, per specimen, after line heating of the 11 to 12 mm thick plates. The analysis results show that the base metal (or parent metal) maintains the original material characteristics in the welds after line heating, considering the permitted tensile strength of 640 to 790 *N*/mm² and elongation rate of 25 %.

3.2 Hardness Test Results of Weld Zones

Figure 4 shows the hardness positions mentioned in the LR-Rule and UR-W28 welding standards [10]. There are total of 44 positions in the upper and lower layers of the welded zones. Additionally, we performed the fine hardness measurement in 0.5 mm intervals to identify whether the brittleness was increasing compared to the base metal (or the parent metal). As shown in Figure 5, the hardness at the HAZ of the weld after line heating was 262.5 Hv10, which was satisfactory compared to the maximum allowable hardness of 420 Hv10. In addition, there was no slight difference in hardness, indicating that no surface freezing occurred. This can be seen as an effect of air cooling without water cooling.

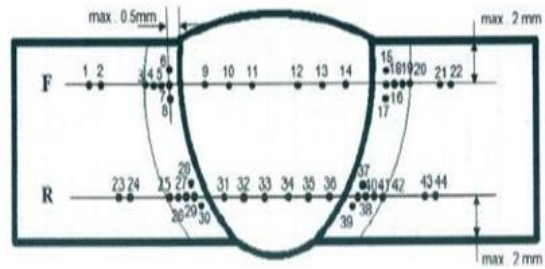

Fig. 4 Hardness check point for butt joint

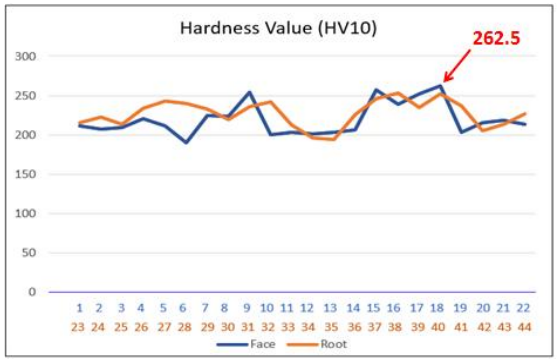

Fig. 5 Hardness value graph for welding butt joint

3.3 Impact Test Results of Weld Zones

The specimens for the impact test were prepared according to ISO 148-1:2016(E) and the impact positions are shown in Figure 6. The specimen sizes were categorized as: (a) Weld Metal, (b) Fusion Line, (c) Fusion Line +1 mm, (d) Fusion Line +3 mm, and (e) Fusion Line +5 mm. This test was performed by loading each of the five test specimens at -196 °C at a gradually increasing distance from the HAZ, following the IGF Code, and the highest required values to achieve the maximum impact value were tested.

Table 6 shows the results that greatly satisfy the maximum impact value requirement of 27 J after line heating for each temperature. This was because the further away from the welds, the greater the impact value. Additionally, the maximum crystal grain formation due to high heat occurred in the weld zones and the HAZs.

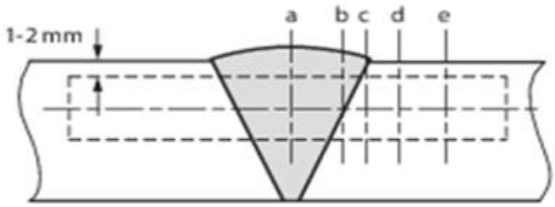

Fig. 6 Impact test location for single V-bevel

Table 6 Tensile test results for welding butt joint

Sample	Test Location	Absorbed Energy (J)			
		1	2	3	Avg
1A-1 (a)	WM (Face)	97.8	84.1	97.8	93.2
1A-2 (b)	FL (Face)	107.2	97.8	111.9	105.6
1A-3 (c)	FL + 1mm	145.6	150.5	165.3	153.8
1A-4 (d)	FL + 3mm	215.3	220.3	245.4	227.0
1A-5 (e)	FL + 5mm	265.2	260.3	289.6	271.7

3.4 Welding Deformation with Temperature

In this study, the integrity of the materials was verified after pre-phase heating through tensile, hardness, and impact tests. Moreover, the trend of temperature variation before and after line heating was examined by thermal analysis. Figure 7 shows the prediction made through analysis indicating that up to 0.87 mm of weld deformation would be generated in the direction of the thickness of the entire test specimen area in the butt weld before line heating. The size of this deformation is determined by the maximum temperature and restraint strength at that point, as the lateral contraction in multi-layer welding initially increases with an increasing amount of welded metal (or deposited metal), but gradually decreases thereafter. This is caused by the gradual increase in strength by which the previously welded metal prevents contraction of the recently welded metal. Factors that significantly affect the amount of lateral contraction

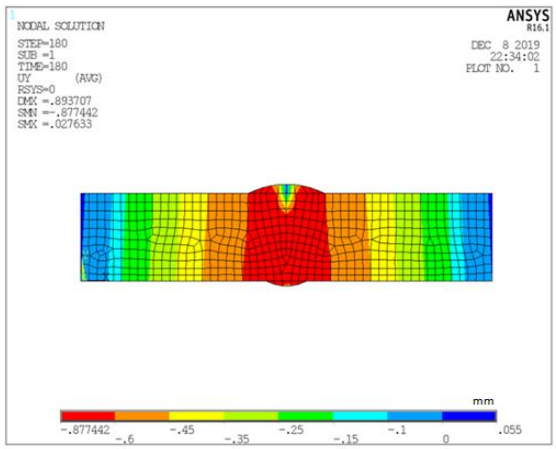

Fig. 7 Distortion of Butt Weld before line heating

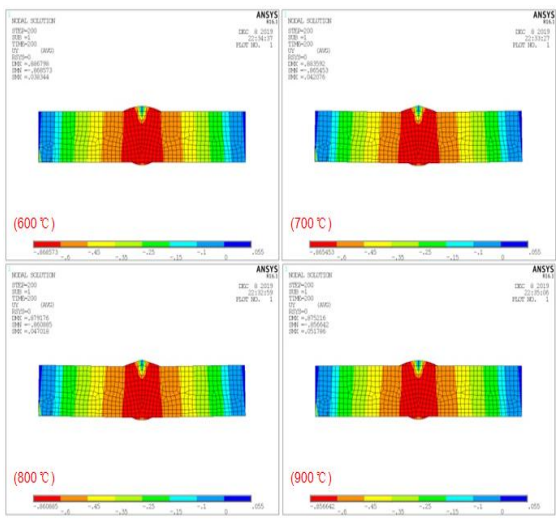

Fig. 8 Temperature distortion for butt weld after line heating

are the distance between the roots and the shapes of the grooves; the wider this gap, the greater the contraction. The single V-shaped bevel forms a larger gap than the double V-shaped bevel, resulting in greater contraction.

Figure 8 shows an analytical model for each temperature-specific weld deformation after line heating. Based on the analytical model, the deformations in the thickness direction caused by heat

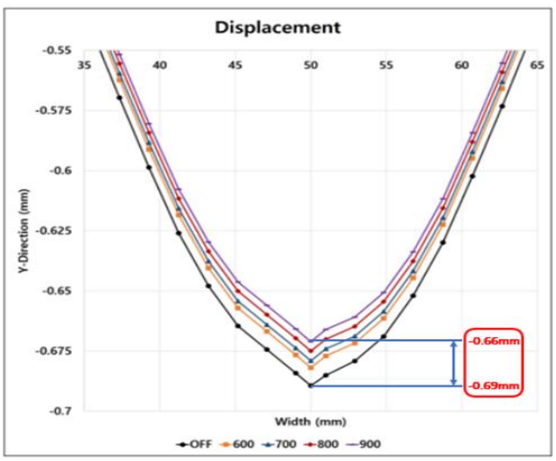

Fig. 9 Graph of distortion due to butt welding before and after line heating

are represented in the graphs as shown in Figure 9. Line heating for each temperature was performed with a reduced deformation caused by elasticity to 0.69 mm from the maximum of 0.87 mm, as mentioned earlier, due to air cooling over time. The maximum deformation before line heating was approximately -0.69 mm, and it was measured as -0.66 mm after line heating at 900 °C. Thus, the deformation was reduced by about 5 % compared to before line heating. It was also confirmed that deformation by welding prior to line heating is reduced in the y-axis direction (mm) of the test specimen under each temperature change condition. The above graph shows the ratios between the plastic deformations of the weld zones and that produced by line heating for each temperature. It was found that pre-heating in the y-axis direction (mm) caused compressive plastic deformation in the opposite direction of the bending deformation of the weld. When the line heating temperature is 900 °C, the plastic region expands compared to that at 600 °C, resulting in a slight reduction in deformation.

4. Conclusion

In this paper, 9 % nickel steel was applied to container ships and weld deformation was studied after line heating for each temperature in the manufacture of type-B LNG fuel tanks. The integrity of this study was ensured by testing within the scope of the applicable standards and regulations of international organizations; furthermore, heat analyses were conducted to determine the optimal line heating temperature, and the following conclusions were drawn.

1. The weld deformation in the thickness direction generated by welding before line heating is up to 0.87 mm. This is similar to what occurs in the welded butt joints of the thick plates used in common shipyards, indicating that 9 % nickel steel can also be worked using line heating methods used for general steel.
2. The analysis model results for each temperature change condition confirmed that the optimal temperature for line heating is 900 °C in the thickness direction.
3. Even after line heating, the results of the tensile, hardness, and impact experiments on the weld zones complied with the permitted values required by international standards.

References

1. Kim, J. T., Chung, H. S., Jeong, H. M., Lee, Kwang. S., "A study on the variation of physical properties of line heated classification DH32 thick plate steel," Journal of the Korean Society of Marine Engineering, Vol. 40, No .9 pp. 774-779, 2016.
2. Choi, Y. H., Lee, Y. W., Choi, K., "Study on tem-perature distribution for various conditions of moving heating source during line heating process," Journal of the Korean Society of Marine Engineering, Vol. 34, No.5 pp. 617-624, 2010.

3. Park, D. H., Jin, H. K., Park, S. S., Shin, S. B., "A study on the prediction of the angular distortion in line heating with high frequency induction heating," Journal of Welding and Joining, Vol. 33, No.1 pp. 80-86, 2015.
4. Jang, C. D., Ko, D. E., Kim, B. I., Park, J. U., "An experimental study of characteristics of plate de-formation by heating process," Journal of the Society of Naval Architects of Korea, Vol. 38, No.2 pp. 62-70, 2001.
5. Kim, J. W., Lee, Y. S., Lee, S. J., Lee, Y. M., Kim, Y. K., " Integrity evaluation of 9% Ni steel Ground LNG Storage Tank by Seismic," Journal of the Society for Computational Design and Engineering, pp. 1205-1205, 2011.
6. Kim, Y. K., Kim, Y. W., Kim, J. H., "Welding Residual Stress and Strength of Thick 9% Nickel Steel Plate," The Korean Society for Power System Engineering, Vol. 18, No. 4, pp.85-90, 2014.
7. Lee, J. S., Kim, S. I., Oh, S. J., “Plate Forming Automation System of Steel Plates by Line Heating Method(1),” Transaction of the Society of Naval Architects of Korea Vol. 31, No. 4, November 1994.
8. Park, J. S., Kim, J., Shin, J. G., Hyun, C. M., Doh, Y. C., Ko, K. H., "Plate Flattening Analysis in Line Heating Process using Bending Strains," Journal of the Society of Naval Architects of Korea, Vol. 45, No.4 pp. 417-425, 2008.
9. Choi, G. Y., Kim, H. J., "A study on Material Properties Exchange due to Line Heating on the Steel Plate," Korea welding society special lecture and conference presentation overview, pp. 84-87, 1989.
10. Lloyd's Register Rule and Regulations - Rule for the Manufacture, Testing ans Certification of Materials, July 2019, incorporating Notice No. 1 & 2 Chapter 12 Welding Qualification tests for steels.